Chapter 3

Numerical Computation

In this chapter the numerical computation of the thermo-elasto-visco-plastic material behaviour as described in the previous chapter is developed. Initially, a detailed description of numerical discretisation approaches with regard to solid mechanical behaviour is presented. Then a theoretical analysis and comparison of the CV-UM vertex based FVM and the Bubnov-Galerkin FEM discretisation techniques is presented. The potential algorithmic approaches are discussed and available time stepping schemes are described. Finally, the linear solvers employed in this research are described and a brief discussion of axisymmetric problems is provided.

3.1 Numerical Discretisation

In this section the necessary numerical discretisation techniques are described from first principles, with particular emphasis on control volume definition. Initially, the governing equations are described in the context of the conservation equations required for a control volume method. Then a general discretisation technique is applied which can lead to either a cell-vertex FVM or a Bubnov-Galerkin FEM. Finally, the FVM control volume technique is applied directly in a standard fashion.

3.1.1 Governing Equations

In the previous chapter, the stress state at a point was described. When considering the complete analysis of stress within a continuum, whether it is a solid or a fluid in motion, the governing equation concerning the conservation of momentum is

$$\nabla.\sigma_{ij} + b_i = \rho a_i, \tag{3.1}$$

which is Cauchy's equation of motion [61], also referred to as the stress equation of small motion [38]. Where b_i is the body force per unit volume, due to gravity for example, a_i is the local acceleration and ρ is the density of the material.

In the research presented here only quasi-static problems are of interest and the acceleration will be considered to be equal to zero. Hence, only the static equilibrium equation will be considered, which is then obtained as

$$\nabla.\sigma_{ij} + b_i = 0. \tag{3.2}$$

Though it should be noted that Demirdžić and Martinović have applied a cell-centred FVM to thermo-mechanical problems on structured meshes involving non-zero accelerations using the conservation equation (3.1) [31]. Hence, indicating that the CV-UM vertex based FVM described in this research will apply generally to such problems.

3.1.2 General Discretisation

In a generalized FEM discretisation treatment an integral formulation is obtained using the method of weighted residuals [107, 52]. This method is also known as the weak formulation of the problem [107, 52].

The method of weighted residuals will be applied to the displacement formulation of the governing equations [108]. In developing the displacement formulation the equations will be described in matrix form. Hence, the governing equilibrium equation (3.2) in matrix form is

$$\mathbf{L^T}\boldsymbol{\sigma} + \mathbf{b} = \mathbf{0} \qquad \text{in } \Omega, \tag{3.3}$$

where $\mathbf{L}$ and $\boldsymbol{\sigma}$ are the linear differential operator and the stress vector, respectively, and are defined in equations (2.16) and (2.18),

$$\mathbf{b^T} = \begin{bmatrix} b_x & b_y & b_z \end{bmatrix}$$

is the body force vector and Ω is the domain volume (or area as the theory applies generally for the two dimensional case with suitably defined matrices and vectors).

To develop the standard displacement formulation, the elastic strain rate defined in equation (2.24) is redefined in vector form as the elastic strain at any instant in time,

$$\boldsymbol{\epsilon}^{el} = \boldsymbol{\epsilon} - \boldsymbol{\epsilon}^{th} - \boldsymbol{\epsilon}^{vp} \tag{3.4}$$

where each strain vector contains six components of the form described in equation (2.16). The constitutive relationship as described in matrix form in equation (2.15) now becomes

$$\boldsymbol{\sigma} = \mathbf{D}\left(\boldsymbol{\epsilon} - \boldsymbol{\epsilon}^{th} - \boldsymbol{\epsilon}^{vp}\right). \tag{3.5}$$

The boundary conditions on the surface $\Gamma = \Gamma_t \cup \Gamma_u$ of the domain Ω can be defined as [107, 71]

$$\mathbf{R^T}\boldsymbol{\sigma} = \mathbf{t_p} \qquad \text{on } \Gamma_t, \tag{3.6}$$

$$\mathbf{u} = \mathbf{u_p} \qquad \text{on } \Gamma_u, \tag{3.7}$$

where $\mathbf{t_p}$ are the prescribed tractions on the boundary Γ_t, $\mathbf{u_p}$ are the prescribed displacements on the boundary Γ_u and

$$\mathbf{R} = \begin{bmatrix} n_x & 0 & 0 \\ 0 & n_y & 0 \\ 0 & 0 & n_z \\ n_y & n_x & 0 \\ 0 & n_z & n_y \\ n_z & 0 & n_x \end{bmatrix} \tag{3.8}$$

is the outward normal operator.

Applying the strain-displacement relationship of equation (2.18) to equation (3.5) and substituting the resulting equation in the traction boundary condition as defined in equation (3.6),

$$\mathbf{R^T}\left(\mathbf{DLu} - \mathbf{D}\boldsymbol{\epsilon}^{th} - \mathbf{D}\boldsymbol{\epsilon}^{vp}\right) - \mathbf{t_p} = \mathbf{0} \qquad \text{on } \Gamma_t, \tag{3.9}$$

and also performing the same substitution on the governing equilibrium equation (3.3):

$$\mathbf{L^T}\left(\mathbf{DLu} - \mathbf{D}\boldsymbol{\epsilon}^{th} - \mathbf{D}\boldsymbol{\epsilon}^{vp}\right) + \mathbf{b} = \mathbf{0} \qquad \text{in } \Omega. \tag{3.10}$$

Applying the method of weighted residuals to equations (3.9) and (3.10), and assuming the displacement boundary conditions as described by equation (3.7) are directly satisfied by the displacement vector $\mathbf{u}$ [107],

$$\begin{aligned}\int_\Omega \mathbf{W^T}\left[\mathbf{L^T}(\mathbf{DLu} - \mathbf{D}\boldsymbol{\epsilon}^{th} - \mathbf{D}\boldsymbol{\epsilon}^{vp})\right] d\Omega \; + \; \int_\Omega \mathbf{W^T b}\, d\Omega \\ + \int_{\Gamma_t} \overline{\mathbf{W}}^{\mathbf{T}}\left[\mathbf{R^T}(\mathbf{DLu} - \mathbf{D}\boldsymbol{\epsilon}^{th} - \mathbf{D}\boldsymbol{\epsilon}^{vp})\right] d\Gamma \; - \; \int_{\Gamma_t} \overline{\mathbf{W}}^{\mathbf{T}}\mathbf{t_p}\, d\Gamma \; = \; \mathbf{0},\end{aligned} \tag{3.11}$$

where $\mathbf{W}$ and $\overline{\mathbf{W}}$ are arbitrary weighting functions. Applying Green's first theorem as defined in Appendix A.2 to the first volume integral term in equation (3.11) and assigning $\mathbf{W} = -\overline{\mathbf{W}}$ without any loss of generality as the weighting functions are completely arbitrary at this point,

$$\begin{aligned}-\int_\Omega [\mathbf{LW}]^{\mathbf{T}}[\mathbf{DLu} - \mathbf{D}\boldsymbol{\epsilon}^{th} - \mathbf{D}\boldsymbol{\epsilon}^{vp}]\, d\Omega \; + \; \int_\Omega \mathbf{W^T b}\, d\Omega \\ + \int_{\Gamma_u} [\mathbf{RW}]^{\mathbf{T}}[\mathbf{DLu} - \mathbf{D}\boldsymbol{\epsilon}^{th} - \mathbf{D}\boldsymbol{\epsilon}^{vp}]\, d\Gamma \; + \; \int_{\Gamma_t} \mathbf{W^T t_p}\, d\Gamma \; = \; \mathbf{0}.\end{aligned} \tag{3.12}$$

It should be noted that the displacement $\mathbf{u}$ has disappeared from the integrals taken along the boundary Γ_t and that the boundary condition as described by equation (3.6) is automatically satisfied. Also, restricting the displacement $\mathbf{u}$ to satisfy the boundary condition as described by equation (3.7) is equivalent to restricting the choice of the weighting function associated with the integral along the boundary Γ_u to be zero [107].

The form of equation (3.12) is the weak form of the equilibrium condition, this is indicated as it permits discontinuous first derivatives of the displacement, which was not permitted in equation (3.11) [52, 107].

At this point the unknown displacement is approximated as [107]

$$\mathbf{u} \simeq \hat{\mathbf{u}} = \sum_{j=1}^{n} \mathbf{N}_j \bar{\mathbf{u}}_j = \sum_{j=1}^{n} \mathbf{I} N_j \bar{\mathbf{u}}_j, \tag{3.13}$$

where $\bar{\mathbf{u}}_j$ is the unknown variable, in this case displacement. N_j is the shape or basis function associated with the unknown displacement, which can be a function of local or

global coordinates. The shape functions utilised in this research are described in Appendix B.9. $\mathbf{I}$ is the third order identity matrix for the three dimensional case.

The displacement approximation can be introduced into equation (3.12) if the arbitrary weighting function $\mathbf{W}$ is replaced by a finite set of prescribed functions [107, 71]

$$\mathbf{W} = \sum_{i=1}^{n} \mathbf{W}_i, \tag{3.14}$$

where $\mathbf{W}_i$ is the weighting function associated with an unknown displacement. Introduction of the displacement approximation into equation (3.12) yields a set of algebraic equations of the following form:

$$\begin{aligned} -\int_{\Omega} [\mathbf{L}\mathbf{W}_i]^{\mathbf{T}} [\mathbf{D}\mathbf{L}\hat{\mathbf{u}} - \mathbf{D}\boldsymbol{\epsilon}^{th} - \mathbf{D}\boldsymbol{\epsilon}^{vp}]\, d\Omega \; + \; \int_{\Omega} \mathbf{W}_i^{\mathbf{T}} \mathbf{b}\, d\Omega \\ + \int_{\Gamma_u} [\mathbf{R}\mathbf{W}]_i^{\mathbf{T}} [\mathbf{D}\mathbf{L}\hat{\mathbf{u}} - \mathbf{D}\boldsymbol{\epsilon}^{th} - \mathbf{D}\boldsymbol{\epsilon}^{vp}]\, d\Gamma \; + \; \int_{\Gamma_t} \mathbf{W}_i^{\mathbf{T}} \mathbf{t_p}\, d\Gamma \; = \; \mathbf{0} \\ \text{for} \qquad i = 1,\, n. \end{aligned} \tag{3.15}$$

It should be noted that the introduction of the displacement approximation introduces the residuals or errors into equation (3.12) and the weighting functions are associated with these residuals or errors. This is the essence of the method of weighted residuals.

The method of weighted residuals outdates the FEM and the latter generally uses local shape or basis functions. As described, the method of weighted residuals always leads to equations of integral form. This integral property is important as the overall system of algebraic equations can be obtained by the summation of contributions from various subdomains. For these reasons, all weighted residual approximations have often been described under the heading of the generalized finite element method [107, 71].

Equation (3.15) can be expressed as a linear system of equations of the form

$$\mathbf{K}\bar{\mathbf{u}} - \mathbf{f} = \mathbf{0}, \tag{3.16}$$

where $\mathbf{K}$ is the global stiffness matrix, $\bar{\mathbf{u}}$ is the global displacement approximation and $\mathbf{f}$ is the global equivalent nodal force vector. $\mathbf{K}$ and $\mathbf{f}$ can be formed from the summation of the following contributions:

$$\mathbf{K}_{ij} \;=\; \int_{\Omega_i} [\mathbf{L}\mathbf{W}_i]^{\mathbf{T}} \mathbf{D}\mathbf{L}\mathbf{N}_j\, d\Omega \; - \; \int_{\Gamma_{u_i}} [\mathbf{R}\mathbf{W}_\mathbf{i}]^{\mathbf{T}} \mathbf{D}\mathbf{L}\mathbf{N}_j\, d\Gamma, \tag{3.17}$$

$$\mathbf{f}_i = \int_{\Omega_i} \mathbf{W}_i^{\mathbf{T}} \mathbf{b}\, d\Omega - \int_{\Omega_i} [\mathbf{LW}_i]^{\mathbf{T}} \mathbf{D}\boldsymbol{\epsilon}^{th} d\Omega - \int_{\Omega_i} [\mathbf{LW}_i]^{\mathbf{T}} \mathbf{D}\boldsymbol{\epsilon}^{vp}\, d\Omega + \int_{\Gamma_{t_i}} \mathbf{W}_i^{\mathbf{T}} \mathbf{t_p}\, d\Gamma + \int_{\Gamma_{u_i}} [\mathbf{RW_i}]^{\mathbf{T}} \mathbf{D}\boldsymbol{\epsilon}^{th} d\Gamma + \int_{\Gamma_{u_i}} [\mathbf{RW_i}]^{\mathbf{T}} \mathbf{D}\boldsymbol{\epsilon}^{vp}\, d\Gamma, \quad (3.18)$$

where Ω_i is the control volume associated with the node i and $\Gamma_i = \Gamma_{u_i} \cup \Gamma_{t_i}$ is the boundary of the control volume.

At this stage, the finite weighting functions have not been specified and the discretisation has been performed in a general fashion. It should be noted that equations (3.17) and (3.18) defining integral control volume contributions to the overall system of equations is significantly different to the standard elemental contributions in the usual FEM discretisation approach.

An important consideration is the possibility that control volumes over which the integral contribution is taken may overlap. Thus, this is not a straight forward integral summation. The assumption is that each finite weighting function removes the residual or error for that individual control volume, thus allowing the summation, as the residual or error over the complete domain must also be removed.

The general discretisation approach described here is vertex based with regard to the control volume. This is a consequence of the application of the boundary conditions to unknowns on the boundary of the domain and associating the unknown with a node as opposed to a cell or element [52]. The specific weighting functions associated with the cell-vertex FVM or the Bubnov-Galerkin FEM can now be applied to equations (3.17) and (3.18).

3.1.2.1 Bubnov-Galerkin FEM

In the Bubnov-Galerkin FEM the weighting function associated with a node is equal to the shape function of the unknown associated with that node [107, 52, 71],

$$\mathbf{W}_i = \mathbf{N}_i.$$

The shape function describes the variation of an unknown over an element and there can be a number of elements associated with each node. Hence, it is apparent that control volumes

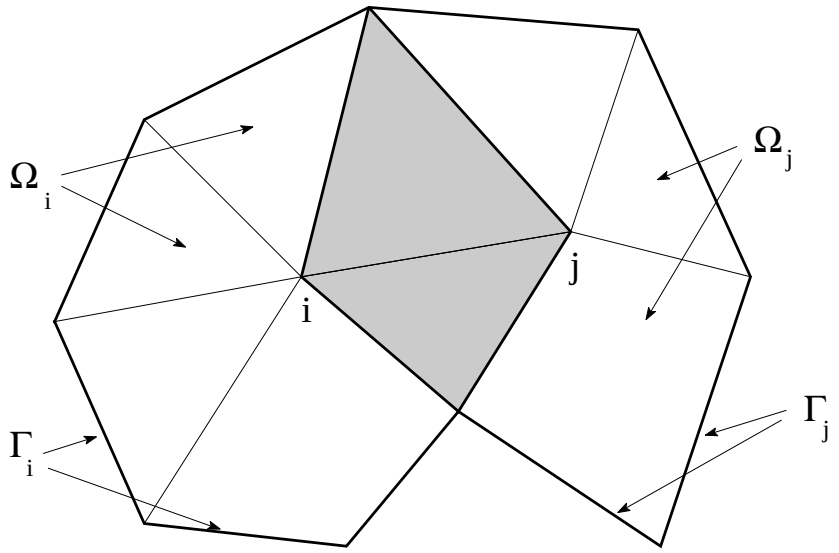

Figure 3.1: Overlapping control volumes in two dimensions.

described by weighting functions of this form will always overlap. This is illustrated in Figure 3.1 for a simple two dimensional case of two adjacent nodes i and j, where the control volumes Ω_i and Ω_j have contributions from all the elements associated with their respective nodes i and j.

Hence, with regard to the Bubnov-Galerkin FEM the contributions to the overall system of equations as described by equations (3.17) and (3.18) are

$$\mathbf{K}_{ij} = \int_{\Omega_i} \mathbf{B}_i^{\mathbf{T}} \mathbf{D} \mathbf{B}_j \, d\Omega, \tag{3.19}$$

$$\mathbf{f}_i = \int_{\Omega_i} \mathbf{N}_i^{\mathbf{T}} \mathbf{b} \, d\Omega - \int_{\Omega_i} \mathbf{B}_i^{\mathbf{T}} \mathbf{D} \boldsymbol{\epsilon}^{th} d\Omega - \int_{\Omega_i} \mathbf{B}_i^{\mathbf{T}} \mathbf{D} \boldsymbol{\epsilon}^{vp} \, d\Omega + \int_{\Gamma_{t_i}} \mathbf{N}_i^{\mathbf{T}} \mathbf{t_p} \, d\Gamma, \tag{3.20}$$

where

$$\mathbf{B}_i = \mathbf{L} \mathbf{N}_i. \tag{3.21}$$

It should be noted that if the boundary of the control volume, such as that described by Γ_i in Figure 3.1, coincides with the external boundary of the domain, the shape functions are not necessarily zero along that part of the boundary. Thus, if a flux is prescribed such as a

traction this will not disappear and is included in the contribution to the equivalent nodal load vector as described in equation (3.20). If the boundary of the control volume does not coincide with the external boundary of the domain, then by definition the weighting function will be zero at these boundaries and the surface integrals will disappear.

It should also be noted that the symmetrical nature of the overall stiffness matrix $\mathbf{K}$ is indicated by equation (3.19). The Bubnov-Galerkin weighting approach is accepted as the optimum technique for treating physical situations described by elliptic or self-adjoint differential equations, as the inherent symmetrical nature is preserved by the choice of weighting functions [107, 71].

3.1.2.2 Cell-vertex FVM

In the cell-vertex FVM the weighting functions associated with a node are equal to unity within the control volume,

$$\mathbf{W}_i = \mathbf{I},$$

and zero elsewhere. In the three dimensional case $\mathbf{I}$ is again the third order identity matrix. This definition is equivalent to that for the subdomain collocation method as defined in the standard texts [52, 107].

However, it should be noted that weighting functions defined in this manner permit a variety of possibilities with regard to the control volume definition. This is because the weighting functions are not restricted to a direct association with the cell or element as in the standard Bubnov-Galerkin case. This is an important consideration and requires the recognition of the cell-vertex FVM as a discretisation technique in its own right [52].

For the cell-vertex FVM the contributions to the overall system of equations as described by equation (3.17) and (3.18) are

$$\mathbf{K}_{ij} = -\int_{\Gamma_{u_i}} \mathbf{R^T D L N}_j \, d\Gamma, \tag{3.22}$$

$$\mathbf{f}_i = \int_{\Omega_i} \mathbf{b} \, d\Omega + \int_{\Gamma_{u_i}} \mathbf{R^T D} \boldsymbol{\epsilon}^{th} d\Gamma + \int_{\Gamma_{u_i}} \mathbf{R^T D} \boldsymbol{\epsilon}^{vp} \, d\Gamma + \int_{\Gamma_{t_i}} \mathbf{t_p} \, d\Gamma. \tag{3.23}$$

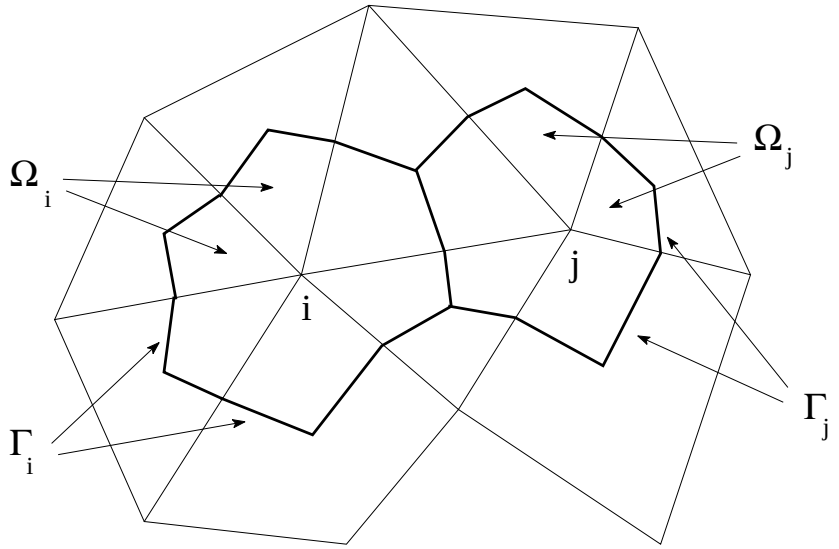

Figure 3.2: Non-overlapping control volumes in two dimensions.

It should be noted that the traction boundary conditions can be applied directly as another surface integral, but in the previous Bubnov-Galerkin FEM an extra surface element is generally included on the domain boundary. However for lower order elements involving linear shape functions this distinction is a minor issue.

An overlapping control volume definition suitable for a cell-vertex FVM in two dimensions is illustrated in Figure 3.1. Alternatively, a non-overlapping cell-vertex FVM in two dimensions is indicated in Figure 3.2. These two techniques have been compared in the numerical solution of one and two dimensional solid mechanics problems involving linear elastic materials [71]. The non-overlapping or CV-UM vertex based FVM proved superior with regard to accuracy and agrees in essence with the standard requirements of conservative control volume methods as given by Patankar [74].

It should be noted from the asymmetric contributions to the overall stiffness matrix as described by equation (3.22) that unlike the Bubnov-Galerkin case the symmetry of the problem cannot be preserved. As mentioned earlier, this is an important issue in solid

mechanics problems, where the differential equations are often elliptical in nature [107, 71]. The accuracy of the Bubnov-Galerkin and the subdomain collocation approach has been reported in many cases and the Bubnov-Galerkin approach is shown to be more accurate [107, 106]. Subdomain collocation techniques equivalent to the cell-vertex FVM and the CV-UM vertex based FVM have been considered [107]. However, in the comparisons of the two methods global shape functions were employed as opposed to local, piecewise, shape functions [107]. The combination of a global shape function and a locally conservative weighting function is not consistent with conservative control volume techniques as described by Patankar [74].

For this reason the cell-vertex FVM was initially argued as being inferior, due to it's theoretical equivalence to the subdomain collocation method, but in the light of further research where different control volume definitions have been proposed such as the CV-UM vertex based FVM, the extent of this inferiority has come into question [71].

3.1.3 Conservative Discretisation

When applying the FV discretisation technique directly, the integral formulation of the conservation equation is discretised directly in physical space [74, 52]. Thus, the integral formulation of the conservation equation (3.2) over a control volume Ω_{cv} is

$$\int_{\Omega_{cv}} (\nabla.\sigma_{ij} + b_i)\, d\Omega = 0 \tag{3.24}$$

and if the divergence theorem as defined in Appendix A.1 is applied to the first integral term on the left then

$$\oint_{\Gamma_{cv}} \sigma_{ij}.n_j d\Gamma + \int_{\Omega_{cv}} b_i d\Omega = 0 \tag{3.25}$$

where n_j is the outward normal and the integration is now applied over the closed surface Γ_{cv}. At this point the conservative nature of the FVM is established as the flux, stress, is integrated over the closed surface Γ_{cv} [43, 42, 4, 31, 48].

From a theoretical mechanics viewpoint, this approach is equivalent to applying the virtual work concept, which is traditionally viewed as the starting point of a Bubnov-Galerkin

FEM [105]. Though in the FVM unit virtual displacements are prescribed, as opposed to arbitrary virtual displacements in the Bubnov-Galerkin FEM [71].

It is now possible to define a collection of discrete control volumes which form the complete solution domain, each of which is independently conservative. These can be cell-centred or cell-vertex control volumes [43, 42, 4, 31, 48]. The CV-UM vertex based FVM will be described in full in the following sections.

It should be noted that in the cell-centred FVM, where in the case of CSM problems the stress, strains and displacements are all stored at the cell centres, a decoupling phenomenon can occur between stress and displacement. This phenomenon is analogous to that which occurs in CFD when the pressure field is decoupled from the velocity field. This similarity allows the solutions to this problem in CSM to be compared with those in CFD. Demirdžić and Martinović [31] have used an approach which is very similar to that of Rhie and Chow [80]. This approach includes a higher order term in the displacement gradient approximation. Whilst, Hattel and Hansen [48] have adopted a staggered grid approach, where a staggered grid is associated with each displacement component and displacements are stored at the cell faces. This is very similar to methods employed in a number of CFD software packages, such as the commercial software package PHEONICS [19].

On the other hand, the cell-vertex FVM stores the displacements at the vertices and stress and strains at the integration points, which can be within the cell or element. The required derivatives are approximated at integration points using the shape function derivatives, this technique will be described in further detail in the following sections. This method inherently avoids the problem of decoupling in the same fashion as the standard Bubnov-Galerkin FEM and is often referred to as partial staggering.

It should also be noted that no distinction has been made between the deformed and undeformed configurations in describing the FVM. This is permissible as an infinitesimal strain approximation is adopted and small displacements are assumed [31].

3.2 Algorithmic techniques

Non-linear problems require special solution techniques. These techniques can be simply viewed as iterative methods, which involve the repeated solution of a linear system of equations, in order to approximate the behaviour of a non-linear relationship.

In the specific case of non-linear material problems a large number of solution techniques are currently available. In the description of the algorithms developed in this research the origin and development of the non-linear solution techniques will be described.

It should be noted that in this research the simpler non-linear solution techniques have initially been implemented, though the approach should apply generally to most non-linear solution techniques.

In this research two algorithmic approaches were initially developed. The first approach follows the more traditional FEM algorithmic approach for non-linear problems, where the displacement variable is solved in a linear whole field fashion for each non-linear iteration. In the second approach the displacement is solved in a non-linear segregated fashion, for each non-linear iteration. This segregated approach was originally applied to two dimensional linear elastic problems by Fryer et al [43]. These two algorithmic approaches are described and compared in the following sections.

3.2.1 Standard non-linear approach

The algorithmic technique adopted in this approach is based upon that of Zienkiewicz and Cormeau [105]. The method can be classified as an initial strain method, which is accepted as being the suitable algorithmic approach for problems involving visco-plastic strains. The implementation of this algorithm in a FVM context for elasto-visco-plastic problems is now described.

The numerical procedure in matrix form is as follows:

(1) Assume known values of the variables $\boldsymbol{\sigma_n}$, $\overline{\mathbf{u}}$, $\boldsymbol{\epsilon_n^{vp}}$ and $\mathbf{f_n}$ at the time instant t_n. Calculate the visco-plastic strain rate using the following relationship obtained from equation 2.21:

$$\dot{\boldsymbol{\epsilon}}_{\boldsymbol{n}}^{\boldsymbol{vp}} = g\{\boldsymbol{\sigma_n}\}.$$

(2) Approximate the visco-plastic strain increment $\Delta\boldsymbol{\epsilon}_{\boldsymbol{n}}^{\boldsymbol{vp}}$ and update t_n as follows:

$$\Delta\boldsymbol{\epsilon}_{\boldsymbol{n}}^{\boldsymbol{vp}} = \dot{\boldsymbol{\epsilon}}_{\boldsymbol{n}}^{\boldsymbol{vp}}\Delta t_n, \quad t_{n+1} = t_n + \Delta t_n.$$

(3) Update the total visco-plastic strain at the current instant in time as follows:

$$\boldsymbol{\epsilon}_{\boldsymbol{n+1}}^{\boldsymbol{vp}} = \boldsymbol{\epsilon}_{\boldsymbol{n}}^{\boldsymbol{vp}} + \Delta\boldsymbol{\epsilon}_{\boldsymbol{n}}^{\boldsymbol{vp}}.$$

(4) Update the load vector with regard to the latest visco-plastic strains using a FVM contribution as described in equation 3.23:

$$\mathbf{f_{n+1}} = \mathbf{p_0} + \int_{\Gamma} \mathbf{R^T D}\boldsymbol{\epsilon}_{\boldsymbol{n+1}}^{\boldsymbol{vp}} \mathrm{d}\Gamma,$$

where $\mathbf{p_0}$ represents the time independent applied loads.

(5) Calculate the associated displacement and stress as follows:

$$\begin{aligned} \overline{\mathbf{u}}_{\mathbf{n+1}} &= \mathbf{K_0^{-1}} \mathbf{f_{n+1}}, \\ \boldsymbol{\sigma}_{\boldsymbol{n+1}} &= \mathbf{D}\left(\boldsymbol{\epsilon}_{\boldsymbol{n+1}} - \boldsymbol{\epsilon}_{\boldsymbol{0}}^{\boldsymbol{th}} - \boldsymbol{\epsilon}_{\boldsymbol{n+1}}^{\boldsymbol{vp}}\right), \\ &= \mathbf{DB}\overline{\mathbf{u}}_{\mathbf{n+1}} - \mathbf{D}\boldsymbol{\epsilon}_{\boldsymbol{n+1}}^{\boldsymbol{vp}}. \end{aligned} \tag{3.26}$$

(6) Return to step (1) and repeat for the next time step with the updated values. The solution has converged if the Euclidian norm ratio of the effective visco-plastic strain rate is within tolerance, i.e.

$$\frac{\|\dot{\epsilon}_n^{eff}\|}{\|\dot{\epsilon}_0^{eff}\|} \times 100 < \text{Tolerance}.$$

The technique utilises an explicit method with regard to time stepping, and this issue will be discussed in detail in the following sections. It is important to note that the FVM only differs from the FEM algorithm in the calculation of the external force vector $\mathbf{f_{n+1}}$ in step (4) and the formulation of the initial stiffness matrix $\mathbf{K_0}$ utilised in step (5). Hence, allowing an accurate comparison of the two methods.

3.2.2 Segregated approach

Initially in this section, the FV formulation as outlined in the previous section will be described in further detail.

Consider equation 3.22 for an arbitrary three dimensional element. It is possible to obtain the complete stiffness matrix $\mathbf{K}_{ij}$ associated with the contributions from the nodes $j = 1, n$ at node i of the element. In three dimensions, this is achieved using the elasticity matrix as described in equation 2.17, the normal operator $\mathbf{R}$ as described in equation 3.8 and the differential operator $\mathbf{L}$ as described in equation 2.18. The shape functions $\mathbf{N}$ are dependent upon the element and are described in Appendix B.

The complete stiffness matrix is then multiplied by the unknown displacement vector $\overline{\mathbf{u}}$ for the element to obtain the following equations:

$$\begin{aligned}
\frac{E}{2(1+\nu)}\Bigg[\frac{2}{1-2\nu}\left((1-\nu)\sum_{i=1}^{n}\frac{\partial N_i}{\partial x}\overline{u}_i+\nu\sum_{i=1}^{n}\left(\frac{\partial N_i}{\partial y}\overline{v}_i+\frac{\partial N_i}{\partial z}\overline{w}_i\right)\right)n_x \\
+\sum_{i=1}^{n}\left(\frac{\partial N_i}{\partial y}\overline{u}_i+\frac{\partial N_i}{\partial x}\overline{v}_i\right)n_y+\sum_{i=1}^{n}\left(\frac{\partial N_i}{\partial z}\overline{u}_i+\frac{\partial N_i}{\partial x}\overline{w}_i\right)n_z\Bigg]\Delta s &= f_{x_i}, \\
\frac{E}{2(1+\nu)}\Bigg[\sum_{i=1}^{n}\left(\frac{\partial N_i}{\partial x}\overline{v}_i+\frac{\partial N_i}{\partial y}\overline{u}_i\right)n_x+\frac{2}{1-2\nu}\Bigg((1-\nu)\sum_{i=1}^{n}\frac{\partial N_i}{\partial y}\overline{v}_i \\
+\nu\sum_{i=1}^{n}\left(\frac{\partial N_i}{\partial x}\overline{u}_i+\frac{\partial N_i}{\partial z}\overline{w}_i\right)\Bigg)n_y+\sum_{i=1}^{n}\left(\frac{\partial N_i}{\partial z}\overline{v}_i+\frac{\partial N_i}{\partial y}\overline{w}_i\right)n_z\Bigg]\Delta s &= f_{y_i}, \\
\frac{E}{2(1+\nu)}\Bigg[\sum_{i=1}^{n}\left(\frac{\partial N_i}{\partial x}\overline{w}_i+\frac{\partial N_i}{\partial z}\overline{u}_i\right)n_x+\sum_{i=1}^{n}\left(\frac{\partial N_i}{\partial y}\overline{w}_i+\frac{\partial N_i}{\partial z}\overline{v}_i\right)n_y \\
+\frac{2}{1-2\nu}\left((1-\nu)\sum_{i=1}^{n}\frac{\partial N_i}{\partial y}\overline{v}_i+\nu\sum_{i=1}^{n}\left(\frac{\partial N_i}{\partial x}\overline{u}_i+\frac{\partial N_i}{\partial z}\overline{w}_i\right)\right)n_z\Bigg]\Delta s &= f_{z_i}. \quad (3.27)
\end{aligned}$$

The integral contributions defined on the LHS of equation 3.27 are performed over each sub-control volume surface, of area Δs, associated with a node.

Similarly, considering equation 3.23 for the three dimensional elasticity matrix, the following contributions to the load vector at node i can be obtained:

$$f_{x_i} = b_x\Delta v+\left[\frac{E}{1-2\nu}\epsilon_{xx}^{th}n_x+\frac{E}{1+\nu}\left[\epsilon_{xx}^{vp}n_x+\frac{1}{2}\epsilon_{xy}^{vp}n_y+\frac{1}{2}\epsilon_{xz}^{vp}n_z\right]+t_{p_x}\right]\Delta s,$$

$$f_{y_i} = b_y \Delta v + \left[\frac{E}{1-2\nu} \epsilon^{th}_{yy} n_x + \frac{E}{1+\nu} \left[\frac{1}{2} \epsilon^{vp}_{yx} n_x + \epsilon^{vp}_{yy} n_y + \frac{1}{2} \epsilon^{vp}_{yz} n_z \right] + t_{p_y} \right] \Delta s,$$

$$f_{z_i} = b_z \Delta v + \left[\frac{E}{1-2\nu} \epsilon^{th}_{zz} n_x + \frac{E}{1+\nu} \left[\frac{1}{2} \epsilon^{vp}_{zx} n_x + \frac{1}{2} \epsilon^{vp}_{zy} n_y + \epsilon^{vp}_{zz} n_z \right] + t_{p_z} \right] \Delta s. \quad (3.28)$$

Here the thermal strains are defined by the linear coefficient of thermal expansion α and the temperature change ΔT as

$$\epsilon^{th}_{xx} = \epsilon^{th}_{yy} = \epsilon^{th}_{zz} = \alpha \Delta T$$

and the following relationship is utilised:

$$\epsilon^{vp}_{xx} + \epsilon^{vp}_{yy} + \epsilon^{vp}_{zz} = 0,$$

which stems from the incompressible nature of the visco-plastic strains. Again the integrations are performed over each sub-control volume surface associated with a node. The body force vector **b** contributions are assembled from sub-control volumes associated with a node.

Equations 3.27 and 3.28 represent the complete formulation of the FVM for a three dimensional elasto-visco-plastic analysis including thermal and mechanical loads and are an extension to the three dimensional elastic formulation of the FVM by Bailey and Cross [4]. With regard to the algorithm described in the previous section the initial stiffness matrix is constructed by contributions from equations 3.27 and the load vector is updated by contributions from equations 3.27. In the two dimensional case similar equations can be obtained using the appropriate matrices associated with a plane stress or strain approximation, which are described in Appendix D. Indeed, a complete two dimensional implementation of the FVM for an elasto-visco-plastic analysis involving a plane stress approximation has been described by Taylor et al [89].

Alternatively, equations 3.27 and 3.28 can be rearranged in a segregated fashion with regard to displacement components. Considering the x component of equations 3.27, it can be rearranged as follows:

$$\frac{E}{2(1+\nu)} \left[\frac{2}{1-2\nu} (1-\nu) \sum_{i=1}^{n} \frac{\partial N_i}{\partial x} \overline{u}_i + \sum_{i=1}^{n} \frac{\partial N_i}{\partial y} \overline{u}_i n_y + \sum_{i=1}^{n} \frac{\partial N_i}{\partial z} \overline{u}_i n_z \right] \Delta s = f'_{x_i}. \quad (3.29)$$

Additionally, the x component of equations 3.27 can be rearranged as

$$f'_{x_i} = b_x \Delta v + \left[\frac{E}{1-2\nu} \epsilon^{th}_{xx} n_x + \frac{E}{1+\nu} \left[\epsilon^{vp}_{xx} n_x + \frac{1}{2} \epsilon^{vp}_{xy} n_y + \frac{1}{2} \epsilon^{vp}_{xz} n_z \right] + t_{p_x} \right] \Delta s$$

$$+\frac{E}{2(1+\nu)}\left[\frac{2}{1-2\nu}\left(\nu\sum_{i=1}^{n}\left(\frac{\partial N_i}{\partial y}\overline{v}_i+\frac{\partial N_i}{\partial z}\overline{w}_i\right)\right)n_x \right. \\ \left. +\sum_{i=1}^{n}\frac{\partial N_i}{\partial x}\overline{v}_i n_y+\sum_{i=1}^{n}\frac{\partial N_i}{\partial x}\overline{w}_i n_z\right]\Delta s. \quad (3.30)$$

The y and z components of equations 3.27 and 3.28 can be also be arranged in similar forms to that of equations 3.29 and 3.30. Thus permitting the solution of the x, y and z components of the displacement vector in a segregated fashion. The segregated solution approach is an extension of the two dimensional approach described by Fryer et al for elastic problems [43, 42]. A two dimensional implementation of the FVM utilizing a segregated solution approach for an elasto-visco-plastic analysis with a plane strain approximation has been described by Taylor et al [90].

In this approach the algorithm described in the previous section is extended within each time step to include a segregated solution approach for the displacement variable. The segregated solution approach for the displacement is based upon the iterative algorithm originally described by Fryer et al for the solution of linear elastic problems [43, 42]. The complete algorithm is defined as follows:

(1) Assume known values of the variables $\boldsymbol{\sigma_n}$, $\overline{\mathbf{u}}$, $\boldsymbol{\epsilon}_{\boldsymbol{n}}^{\boldsymbol{vp}}$ and $\mathbf{f_n}$ at the time instant t_n. Calculate the visco-plastic strain rate using the following relationship obtained from equation 2.21:

$$\dot{\boldsymbol{\epsilon}}_{\boldsymbol{n}}^{\boldsymbol{vp}} = g\{\boldsymbol{\sigma_n}\}.$$

(2) Approximate the visco-plastic strain increment $\Delta\boldsymbol{\epsilon}_{\boldsymbol{n}}^{\boldsymbol{vp}}$ and update t_n as follows:

$$\Delta\boldsymbol{\epsilon}_{\boldsymbol{n}}^{\boldsymbol{vp}} = \dot{\boldsymbol{\epsilon}}_{\boldsymbol{n}}^{\boldsymbol{vp}}\Delta t_n, \quad t_{n+1} = t_n + \Delta t_n.$$

(3) Update the total visco-plastic strain at the current instant in time as follows:

$$\boldsymbol{\epsilon}_{\boldsymbol{n+1}}^{\boldsymbol{vp}} = \boldsymbol{\epsilon}_{\boldsymbol{n}}^{\boldsymbol{vp}} + \Delta\boldsymbol{\epsilon}_{\boldsymbol{n}}^{\boldsymbol{vp}}.$$

(4) Construct the associated coefficient matrix $\mathbf{A}$ for the displacement component $\boldsymbol{\phi}$ and the load vector $\mathbf{b}$ using equations 3.29 and 3.30 respectively, and solve using the correction format

$$\mathbf{A}\boldsymbol{\phi}^{\boldsymbol{c}} = \mathbf{b} - \mathbf{A}\boldsymbol{\phi}^{old},$$

where $\boldsymbol{\phi}^{new} = \boldsymbol{\phi}^{old} + \boldsymbol{\phi}^{\mathbf{c}}$.

(5) Return to step (4) and repeat for each displacement component.

(6) Return to step (4) and repeat for the next global iteration. The displacement solution has converged if the error norms and the residual norms for all the displacement components are within the convergence criterion.

$$Max\,(ENORM,\ RNORM) \leq Tolerance.$$

(7) Calculate the stress associated with the whole displacement vector $\overline{\mathbf{u}}$ assembled from each displacement component $\boldsymbol{\phi}$

$$\begin{aligned} \boldsymbol{\sigma}_{\boldsymbol{n+1}} &= \mathbf{D}\left(\boldsymbol{\epsilon}_{\boldsymbol{n+1}} - \boldsymbol{\epsilon}_{\mathbf{0}}^{\boldsymbol{th}} - \boldsymbol{\epsilon}_{\boldsymbol{n+1}}^{\boldsymbol{vp}}\right), \\ &= \mathbf{DB}\overline{\mathbf{u}}_{\mathbf{n+1}} - \mathbf{D}\boldsymbol{\epsilon}_{\boldsymbol{n+1}}^{\boldsymbol{vp}}. \end{aligned} \tag{3.31}$$

(8) Return to step (1) and repeat for the next time step with the updated values. The solution has converged if the Euclidian norm ratio of the effective visco-plastic strain rate is within tolerance, i.e.

$$\frac{\|\dot{\epsilon}_n^{eff}\|}{\|\dot{\epsilon}_0^{eff}\|} \times 100 < \text{Tolerance}.$$

3.2.3 Time stepping schemes

The algorithms described in this section have employed an explicit time stepping scheme. This is consistent with the original FE algorithm as originally described and employed by Zienkiewicz and Cormeau [105], upon which the previously described FV algorithms are based. Alternatively, the methods employed in developing the FV algorithms will apply generally to the implicit methods employed in the FE algorithms for the solution of elasto-visco-plastic problems as described by Owen and Hinton [72]

3.2.3.1 Estimation of time step length

The estimation of the time step length is an important consideration with regard to the performance of the algorithms. The time step limit must be limited in order to both preserve

numerical stability of the time integration process and to ensure solution accuracy. The methods associated with the original FE algorithm of Zienkiewicz and Cormeau [105] have been adopted in the FV algorithms and are described in the following sections.

3.2.3.2 Analytical estimation

A theoretical restriction on a fixed time step length can be derived for an elasto-visco-plastic formulation. The derivation involves the analysis of the formulation as a non-linear system of first order differential equations and was originally performed by Cormeau [23] with regard to a FE algorithm.

The derived limit ensures the stability of the solution and is dependent upon the material properties as follows:

$$\Delta t \leq \frac{4(1+\nu)}{3\gamma E}. \tag{3.32}$$

3.2.3.3 Empirical estimation

A variable time step can be obtained empirically for each interval of integration [105, 81]. The time step limit must be limited in order to both preserve numerical stability of the time integration process and to ensure solution accuracy. The magnitude of the time step is controlled by a factor τ which limits the maximum effective visco-plastic strain increment $\Delta\epsilon_n^{evp}$ as a fraction of the total effective strain ϵ_n^{eff} which implies

$$\Delta t \leq \tau \left[\frac{\epsilon_n^{eff}}{\dot{\epsilon}_n^{evp}} \right]_{min}. \tag{3.33}$$

The minimum is found over all integration points associated with an element in the structure or component. The value τ is empirically defined and for explicit time stepping schemes experience suggests values in the range $0.01 < \tau < 0.1$. Additionally, experience suggests that the change in time step length between any two integration intervals is limited to

$$\Delta t_{n+1} \leq 1.5\Delta t_n.$$

For many problems the choice of time step calculation is not a major issue. In general the empirical scheme is more robust and handles problems involving a number of materials without any extra consideration and is generally employed throughout this research.

3.3 Linear solvers

At this point it is important to note that the two algorithmic approaches described in this Chapter furnish differently conditioned matrices as associated with the linear system of equations to be solved.

For the segregated algorithmic approach the matrices are always diagonally dominant and fully iterative linear solvers, such as the Gauss-Seidel (GS) and Successive Over Relaxation (SOR) solution procedures [9], can be employed. Alternatively, semi-direct solvers can be employed. Hence, the Conjugate Gradient Method (CGM) and the BiConjugate Gradient Method (BiCGM) [9] can be employed when the matrices are symmetric and asymmetric, respectively. In both cases it is possible to precondition the matrices to improve the efficiency of the particular solver employed [42, 43].

For the whole field algorithm the matrices are not generally diagonally dominant and fully iterative procedures are not practical [9]. For this reason the above described semi-direct solvers are employed. It is also important to note that the FEM employed in this research will always furnish a symmetric matrix and a CGM solver can always be employed.

It is also important to note that a compacted storage technique is employed for the sparse matrices encountered in this research and the linear solvers are modified accordingly [9].

3.4 Axisymmetric problems

For a number of CSM problems involving cylindrical polar (r, θ, z) coordinates it is possible to assume the solution is invariant in the hoop or θ direction, which leads to axial symmetry

about the z axis.

Considering the axisymmetric stress equilibrium equations [38]

$$\begin{aligned} \frac{\partial \sigma_{rr}}{\partial r} + \frac{\partial \sigma_{rz}}{\partial z} - \frac{\sigma_{rr} - \sigma_{\theta\theta}}{r} &= 0, \\ \frac{\partial \sigma_{zr}}{\partial r} + \frac{\partial \sigma_{zz}}{\partial z} - \frac{\sigma_{zr}}{r} &= 0. \end{aligned}$$

Where body forces are neglected.

It is possible, using the following expressions:

$$\begin{aligned} \frac{1}{r}\frac{\partial \left(r\sigma_{rr}\right)}{\partial r} &= \frac{1}{r}\frac{r\partial \sigma_{rr}}{\partial r} + \frac{\sigma_{rr}}{r}, \\ \frac{1}{r}\frac{\partial \left(r\sigma_{rz}\right)}{\partial r} &= \frac{1}{r}\frac{r\partial \sigma_{rz}}{\partial r} + \frac{\sigma_{rz}}{r}, \end{aligned}$$

to rearrange the equilibrium equations as

$$\begin{aligned} \frac{1}{r}\frac{\partial \left(r\sigma_{rr}\right)}{\partial r} + \frac{\partial \sigma_{rz}}{\partial z} - \frac{\sigma_{\theta\theta}}{r} &= 0, \\ \frac{1}{r}\frac{\partial \left(r\sigma_{zr}\right)}{\partial r} + \frac{\partial \sigma_{zz}}{\partial z} &= 0. \end{aligned}$$

Integrating the above equations over a control volume bounded by the closed curve c and then applying Stokes's theorem (in the plane) as described in Appendix A.3, to the first two terms in both the above equations furnishes,

$$\begin{aligned} \oint_c \left(r\sigma_{rr}\,dz - r\sigma_{rz}\,dr\right) - \iint \sigma_{\theta\theta}\,drdz &= 0, \\ \oint_c \left(r\sigma_{zr}\,dz - r\sigma_{zz}\,dr\right) &= 0. \end{aligned}$$

It is now apparent that a considerable disadvantage of the FVM should be noted, when compared to the standard FEM, for axisymmetric problems. The disadvantage arises as it is not possible to transform all the integral terms in the above equations from surface integrals to line integrals, hence complicating the FVM.

This point is further illustrated when comparing the FVM and the FEM with regard to matrix formulations. In Appendices D.2 and D.5 the elasticity matrix and the differential operator associated with the standard FEM, when applied to axisymmetric problems are

described, respectively, but it is not possible when applying standard control volume techniques to derive a corresponding normal operator matrix as required by the FVM described here.

This complication was discussed by Fryer [42] with regard to a segregated algorithmic approach and a hybrid numerical scheme involving line and surface integrals was employed, with the surface integrals appearing as additional source terms [42]. This was feasible as the originally linear elastic problem was solved in a non-linear fashion, when the segregated algorithmic approach was employed [42].

Conversely, when the whole field algorithmic approach is employed the same technique was not possible as the whole displacement field is solved in one linear iteration. For this reason it was not possible to include the axisymmetric approximation in the general description and formulation of the FVM with regard to the whole field algorithm.

3.5 Closure

In this chapter, the essential differences of the FVM and the FEM have been highlighted with regard to numerical algorithms for the solution of mechanical problems involving material non-linearity. Additionally, two FV algorithmic approaches have been described, a whole field displacement and a segregated displacement technique.

The algorithms described in this chapter will be applied to a variety of mechanical problems in the following chapters in order to compare their suitability.